GOCE High Level Processing Facility

External calibration of GOCE SGG data with terrestrial gravity data

Doc. No.: GO-TN-HPF-GS-0070
Issue: 1
Revision: 1
Date: 03 / 11 / 2005

Prepared by: The European GOCE Gravity Consortium
EGG-C

Document Information Sheet

Document Name
External calibration of GOCE SGG data with terrestrial gravity data

Document ID	Issue	Date
GP-TN-HPF-GS-0070	1.1	07/10/2004

Author	Institute
D. Arabelos C.C. Tscherning	UCPH (visiting from University of Thessaloniki) UCPH
Contributions from	Institute

Document Category	Document Class	Document Level
3	R	3

Configuration Item		Confidentiality Level

Appropriate Signatures		
Name	signature	Signature for approval
		YES/ NO

Distribution List	
Person	Institute
R. Floberghagen, D. Muzi, M. Mezzadri	ESA/ESTEC
R. Rummel, Th. Gruber	IAPG
R. Koop, M. Hofhuis	SRON
EGG-c partners	

List	
DIL	YES
CDL	NO
CIDL	YES
CSL	NO
CCN	NO
SWPRL	NO

Data Package	
SRR	NO
ADIR	NO
CDR	NO
AR0	NO
AR 1	NO
AR 2	NO

Document Change Record

ISSUE /REV.	CLASS (R=Review /A=Approval)	DATE	REASON FOR CHANGE	CHANGED PAGES / PARAGRAPHS
1.0	R	07/10/2004	New report that describes the activities for HPF WP3220	All
1.1		2005-11-03	Revision after review	All

Abbreviations and Acronyms

AD	Applicable Document
ADD	Architectural Design Document
ADIR	Architectural Design and Interface Review
ADP	Auxiliary Data Provider
AIT	Acceptance, Integration, Test
AO	Announcement of Opportunity
AR	Acceptance Review
AS	Anti-Spoofing
ATP	Authorisation To Proceed
ATR	Algorithm Test Review
CAB	Change Appeal Board
CBCP	Current Baseline Cost Plan
CCN	Contract Change Notice
CDAF	Command and Data Acquisition Facility
CDP	Configuration and Documentation management Plan
CDR	Critical Design Review
CFI	Customer Furnished Item
CHAMP	CHAllenging Minisatellite Payload for geophysical research and application
CMF	Calibration and Monitoring Facility
CNL	Contract change Notices status List
COP	Commissioning Operations Phase
COS	Consortium Organisation Structure
CPF	Central Processing Facility
CPR	Cycle Per Revolution
CPS	Company Project Structure
CR	Change Request
CRB	Change Review Board
DCN	Document Change Notice
DDP	Design and Development Plan
DFACS	Drag-Free and Attitude Control System
DPA	Data Processing Archive
DPM	Detailed Processing Model
DSAT	Development Site Acceptance Test
DTL	Documentation Tree and status List
E2E	End-to-End Simulator
ECMWF	European Centre for Medium-range Weather Forecast
ECP	External Calibration Products
ECSS	European Cooperation for Space Standardization
EFRF	Earth Fixed Reference Frame
EGG	Electrostatic Gravity Gradiometer
EGG-C	European GOCE Gravity Consortium
EGM96	Earth Gravity Model 1996
EM	Engineering Model
EME2000	Equinox and Mean Equator of J2000.0
EO	Earth Observation
EOEP	Earth Observation Envelope Programme
EPAR	Extended mission Product Acceptance Review
ESA	European Space Agency
FM	Flight Model
FOCC	Flight Operations Control Centre
FOS	Flight Operations Segment
GLONASS	GLObal NAvigation Satellite System
GOCE	Gravity field and steady-state Ocean Circulation Explorer
GPS	Global Positioning System
GRACE	Gravity Recovery And Climate Experiment
GRF	Gradiometer Reference Frame
GS	Ground Segment
GSOV	Ground Segment Overall Validation
GSRR	Ground Segment Readiness Review
HK	House-Keeping
HOP	Hibernation Operations Phase
HPF	High level Processing Facility
HW	Hardware
IAG	International Association of Geodesy
ICD	Interface Control Document
IGS	International GPS Service
ILRS	International Laser Ranging Service
IPF1	Instrument Processing Facility level 1
ISP	Instrument Source Packet
ITT	Invitation To Tender
L	Level, L-band frequency
LAN	Local Area Network
LEOP	Launch and Early Orbit Phase
LORF	Local Orbital Reference Frame
LRR	Laser Retro-Reflector
LSC	Least Squares Collocation
LTA	Long-Term Archive
MBW	Measurement BandWidth
MOP	Measurement Operational Phase
MPS	Mission Planning System
NA	Not Applicable
NRT	Near-Real Time

OBCP	On-Board Control Procedures
OBT	On-Board Time
ORR	Operational Readiness Review
OSAT	On-Site Acceptance Test
PAR	Product Acceptance Review
PCD	Product Confidence Data
PDD	Product Definition Document
PDS	Payload Data Segment
PF	Processing Facility
PI	Principal Investigator
POD	Precise Orbit Determination
PSD	Packet Structure Definition; Power Spectral Density
QL	Quick-Look
QLP	Quick-Look Products
RD	Reference Document
RERF	Radial Earth-pointing Reference Frame
RFQ	Request For Quotation
RMS	Root-Mean Square
RPF	Reference Planning Facility
RSS	Root-Sum Square
S/C	Space-Craft
SCP	Secure Copy (remote file copy program)
SDE	Software Development Environment
SFTP	Secure File Transfer Program
SGG	Satellite Gravity Gradiometer
SLR	Satellite Laser Ranging
SMF	Software Maintenance Facility
SOW	Statement Of Work
SPC	Satellite Prime Contractor
SPF	Sub-Processing Facility
SPR	Software Problem Report
SPRL	Software PRoblems status List
SRD	System Requirements Document
SRR	System Requirements Review
SST	Satellite-to-Satellite Tracking
SSTI	Satellite-to-Satellite Tracking Instrument
SSTR	Sub-System Test Review
STP	Software Test Plan
SVT	System Validation Test
SW	SoftWare
SWRD	SoftWare Requirements Document
TBC	To Be Confirmed
TBD	To Be Defined
TC	TeleCommand
TM	TeleMetry
TP	Test Plan
TR	Test Report
USF	User Services Facility
UTC	Universal Time Coordinated
V0/1/2	Version 0/1/2
VC	Virtual Channel
WAN	Wide Area Network
WBS	Work Breakdown Structure
WP	Work Package
XML	eXtensible Markup Language

Table of Contents

1. INTRODUCTION

1.1 PURPOSE AND SUMMARY

The purpose of this document is to describe the tests that have been performed in the context of HPF WP3220. WP3220 deals with the external calibration of GOCE SGG data with terrestrial data. In this report, terrestrial gravity anomalies were selected from three extended continental regions, having a smooth gravity field, in order to determine the appropriate size of the area for gravity data collection as well as the required data-sampling for calibration of the GOCE satellite gravity gradient (SGG) data. Using Least Squares Collocation (LSC), prediction of gravity gradient components was carried out at points on a realistic orbit of the IAG SC7 simulated data set. Based on the mean error estimation it was shown that up to 80% of the signal of the gravity gradient components, as it is expressed through the covariance function of the terrestrial gravity data, can be recovered in the case of an optimal size of the collection area and of the optimum resolution of the data. These optimal conditions, e.g. for the Australian gravity field, correspond to a 10^0 x 12^0 area extent and a 5' data-sampling.

1.2 APPLICABILITY

This document is part of the Deliverable Items List [AD-3]. The first issue is delivered at PM2 and classifies for review by the Agency. An update of the document shall be delivered as needed. This document applies to the development phase and to the actual implementation and operational phases of the HPF.

1.3 DEFINITIONS

The term "Contract" is used to indicate the HPF implementation contract.
The term "the Contractor" is used to indicate the entity in charge of implementing the HPF.
The term "Agency" is used to indicate the European Space Agency (ESA).

EGG-C is composed by 10 European institutions. Institutions and team members contributing to the HPF project are defined in Table 1-1.

Table 1-1: EGG-C Team Members in Alphabetical Order

Acronym	Institution	Function	Team Members
AIUB	Astronomical Institute, University of Bern, Switzerland	WP4000 Partner	G. Beutler U. Hugentobler
CNES	Centre National d'Etudes Spatiales, Groupe de Recherche de Géodésie Spatiale, Toulouse, France	WP5000 Manager	G. Balmino S. Bruinsma
FAE/A&S	Faculty of Aerospace Engineering, Astrodynamics & Satellite systems, Delft University of Technology, Delft, The Netherlands	WP 4000 Manager WP 3000 Partner WP 8000 Partner WP 6000 Consultant	P. Visser
GFZ	GeoForschungsZentrum Potsdam, Department 1 Geodesy and Remote Sensing, Potsdam, Germany	WP 5000 Partner	Ch. Reigber P. Schwintzer
IAPG	Institute of Astronomical and Physical Geodesy, Technical University Munich, Germany	Principal Investigator Management WP 3000 Partner WP 4000 Partner WP 6000 Partner WP 8000 Manager	R. Rummel Th. Gruber J. Flury
ITG	Institute of Theoretical Geodesy, University Bonn, Germany	WP 6000 Partner	W.D. Schuh
POLIMI	DIIAR – Sezione Rilevamento, Politecnico di Milano, Italy	WP 7000 Manager	F. Sanso F. Migliaccio
SRON	SRON National Institute for Space Research , Utrecht, The Netherlands	Management WP3000 Manager	R. Koop J. Bouman
TUG	Institute of Navigation and Satellite Geodesy, Graz University of Technology	WP 6000 Manager	H. Sünkel R. Pail G. Plank
UCPH	Department of Geophysics, University of Copenhagen, Denmark	WP 3000 Partner WP 7000 Partner	Ch. Tscherning

2. APPLICABLE AND REFERENCE DOCUMENTS

2.1 APPLICABLE DOCUMENTS

[AD-1] GO-SW-ESA-GS-0079: GOCE High Level processing Facility, Statement of Work, Issue 1.0, 5. December 2003
[AD-2] GO-RS-ESA-GS-0080: GOCE High Level processing Facility, Statement of Work Appendix 1, Management Requirements, Issue 1.0, 5. December 2003
[AD-3] GO-LI-ESA-GS-0081: GOCE High Level Processing Facility, Statement of Work Appendix 2, Deliverable Items List, Issue 1.0, 5. December 2003
[AD-4] GO-RS-ESA-GS-0082: GOCE High Level Processing Facility, Statement of Work Appendix 3, Technical Requirements Specification, Issue 1.0, 5. December 2003
[AD-5] GO-LI-ESA-GS-0087: GOCE High Level Processing Facility, Statement of Work Appendix 4, List of CFI, Issue 1.0, 5. December 2003
[AD-6] GO-TN-ESA-GS-0085: GOCE High Level Processing Facility, Statement of Work Appendix 5, Tailoring of ECSS Standards, Issue 1.0, 5. December 2003
[AD-7] ECSS-E-40B: Space Engineering, Software Standards, Draft Issue, 28. July 2000
[AD-8] ECSS-Q-80B: Space Product Assurance, Software Product Assurance, Issue 3. April 2000
[AD-9] PE-TN-ESA-GS-0001: Earth Explorer Ground Segment File Format Standard
[AD-10] GO-ID-ACS-GS-0109: PDS Product Specification Document
[AD-11] GO-IC-AI-0009: End-to-End Simulator Post-Processing
[AD-14] GO-ID-ACS-GS-0111: PDS-HPF Interface Control Document: L2, QL and External Calibration Products

As a general rule it holds that the latest approved issue of the document is applicable, except if the issue number and the document date is specified.

2.2 REFERENCE DOCUMENTS

[RD-1] ESA-SP-1233(1): Gravity Field and Steady-State Ocean Circulation Mission
[RD-2] GO-RS-ESA-SY-0001: GOCE Mission requirements Document
[RD-3] GO-TN-ESA-GS-0017: GOCE Ground Segment Concept and Architecture
[RD-4] GO-SP-AI-0004: GPS Receiver Ground Processing Algorithms Specification
[RD-5] GO-SP-AI-0003: Gradiometer Ground Processing Algorithms Specification
[RD-6] GO-TN-AI-0067: Gradiometer Ground Processing Algorithms Documentation
[RD-7] GO-TN-AI-0068: Gradiometer Ground processing Analysis
[RD-8] GO-PL-AI-0039: Gradiometer Calibration Plan
[RD-9] GO-TN-AI-0069: Gradiometer On-Orbit Calibration Procedure Analysis
[RD-10] GO-RP-AI-0014: Mission Analysis Report
[RD-11] CS-MA-DMS-GS-0001: Earth Explorer Mission Conventions Document
[RD-12] GO-MA-AI-0002: GOCE User's Manual
[RD-13] GO-TN-AI-0027: Performance Requirements and Budgets for the Gradiometric Mission

[RD-14] GO-TN-IAPG-0001: Detailed Processing Model for EGG
[RD-15] GO-TN-IAPG-0002: Detailed Processing Model for SSTI
[RD-16] GO-ID-ESC-FS-5070: FOS/PDS – PDS/SLR: Predicted Orbit File
[RD-17] GO-RS-ESA-GS-0052: Product Requirement Document
[RD-18] ECSS-M-00A: Policy Principles
[RD-19] ECSS-M-10A: Project Breakdown and Structures
[RD-20] ECSS-M-20A: Project Organization
[RD-21] ECSS-M-30A: Project Phasing and Planning
[RD-22] ECSS-M-40A: Configuration Management
[RD-23] ECSS-M-50A: Information / Documentation Management
[RD-24] ECSS-M-60A : Cost Schedule Management
[RD-25] ECSS-M-70A: Integrated Logistics Support
[RD-26] GO-MI-ESA-0101: Minutes of the HPF Negotiation Meeting
[RD-27] GO-AI-HPF-GS-0008: Action Item Reply of HPF Negotiation Meeting
[RD-28] GO-AI-HPF-GS-0013: Action Item Reply of HPF Negotiation Meeting
[RD-29] Arabelos, D. and C.C. Tscherning, 1998, Calibration of satellite gradiometer data aided by ground gravity data. JoG, 72, 617-625
[RD-30] Bouman, J., R. Koop, C.C.Tscherning and P.Visser (2004): Calibration of GOCE SGG Data Using High-Low SST, Terrestrial Gravity data, and Global Gravity Field Models. Journal of Geodesy, 78, no. 1 -2. DOI 10.1007/s00190-004-383-5
[RD-31] Howe, E., L.Stenseng and C.C.Tscherning: Analysis of one month of CHAMP state vector and accelerometer data for the recovery of the gravity potential. Advances in Geosciences, (2003), 1, p. 1-4, 2003
[RD-32] Moritz, H.: Advanced Physical Geodesy, 1980
[RD-33] Torge, W.: Geodesy, 3. ed., 2001
[RD-34] Tscherning, C.C.: Testing frame transformation, gridding and filtering of GOCE gradiometer data by Least-Squares Collocation using simulated data. In print proceedings IAG General Assembly, Sapporo July 2003
[RD-35] Tscherning, C.C., R.Forsberg and P.Knudsen: The GRAVSOFT package for geoid determination. Proc. 1. Continental Workshop on the Geoid in Europe, Prague, May 1992, pp. 327-334, Research Institute of Geodesy, Topography and Cartography, Prague, 1992.

3. GOCE GROUND SEGMENT

3.1 OVERVIEW GOCE GROUND SEGMENT

The GOCE ground segment concept and architecture is described in [RD-3]. The following gives a brief summary of all ground segment elements, depicted in Figure 3-1.

Figure 3-1: GOCE Ground System

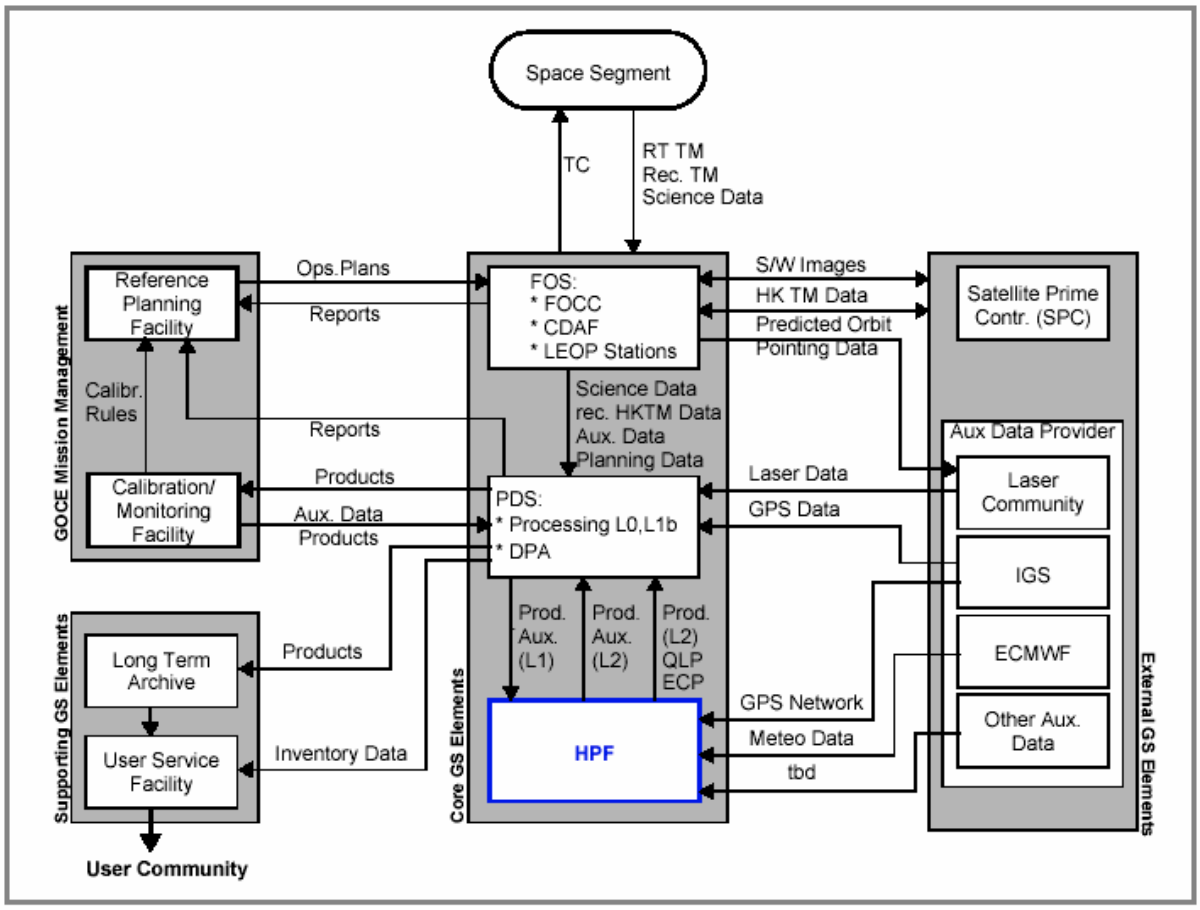

3.2 HIGH-LEVEL PROCESSING FACILITY

Within the GOCE GS the HPF is one of the Core GS Elements (ESA-controlled), and it is charged with the generation of L2 products and acquisition of the external (auxiliary) data needed to generate these products, the delivery of these products (auxiliary, intermediate and final) to the PDS/DPA and/or the LTA and the generation of QLP and ECP for the purpose of the activities of the CMF.

4. OVERVIEW

In the last decade numerous investigations were published, concerning the calibration of GOCE satellite gravity gradiometer data, (e.g. [RD-30]: Bouman et al, 2004). The use of Least Squares Collocation (LSC) ([RD-32]: Moritz, 1980, [RD-33]: Torge, 2001) as an element of the space-wise approach methods has also been discussed in a number of papers (e.g. [RD-34]: Tscherning 2003). The aim of this work was to determine the size of required areas with terrestrial gravity data, as well as the required resolution and accuracy of the gravity data for calibration when LSC is used. The aim is to detect possible systematic errors in the GOCE SGG data.

An observed gravity gradient y_i associated with the anomalous potential T through a linear functional L_i may be expressed through the equation

$$y_i = L_i(T) + e_i + A_i^T \cdot X \qquad (1)$$

with

- Parameters X equal to bias, tilt and contingently scale factor for each observation and each track or part of a track.
- A_i = 1 if bias only present
- A_i = time-difference if tilt/drift is present
- $A_i = L_i(V)$ (full potential) if scale-factor present.

Then an estimate of T and of the parameters X are obtained as

$$\widetilde{T}(P) = \{C_{pi}\}^T \overline{C}^{-1}(y - A^T X) \qquad (2)$$

$$\overline{X} = (A^T \overline{C}^{-1} A + W)^{-1} A^T \overline{C}^{-1} y) \qquad (3)$$

where W is the a-priori weight matrix for the parameters (generally the zero matrix), C_{Pi} is the covariance between the i-th observation and the value of T in a point P and $\overline{C}$ the variance covariance of the observations with the error-covariances D added.

$$\overline{C} = C + D \qquad (4)$$

$$C_{ij} = COV(L_i, L_j) = L_i(L_j(COV(T(P), T(Q)) \qquad (5)$$

The observation vector y may contain any combination of ground and satellite data.

Predicted values are obtained by applying the associated linear functional (L) on the estimate of T. Error estimates may also be computed. The mean square error of the parameter vector becomes

$$m_X^2 = (A^T \overline{C}^{-1} A + W)^{-1} \qquad (6)$$

and using

$$H = \{COV(L, L_i)\}^T \overline{C}^{-1} \tag{7}$$

the mean square error of an estimated quantity $L(\tilde{T})$ (such as T_{zz}) will be

$$m_L^2 = \sigma_L^2 - H\{\mathrm{cov}_{(L, L_i)}\} + H\, A m_X^2 (HA)^T . \tag{8}$$

The (signal) covariance function is expressed as a Legendre series in two parts, equivalent to using a reference field with appropriate error-degree-variances σ_i^e, P_i are Legendre polynomials, ψ the spherical distance between P and Q and r, r' are the radial distances of P, Q respectively from the origin. a is a constant and N=360 since we are using EGM96 to this degree.

$$\begin{aligned} COV(T(P), T(Q) = COV(\psi, r, r') = \sum_{i=2}^{N} \sigma_i^e \left(\frac{R^2}{rr'}\right)^{i+1} P_i(\cos\psi) \\ + \sum_{i=N+1}^{\infty} \frac{a}{(i-1)(i-2)(i+4)} \left(\frac{R^2}{rr'}\right)^{i+1} P_i(\cos\psi) \end{aligned} \tag{9}$$

Hence least-squares collocation with parameters may be used to combine ground gravity and GOCE gravity gradients and to determine related physical parameters and their error-estimates. The above equations have been implemented in the GRAVSOFT (Tscherning et al., 1992, Tscherning, 2003) program GEOCOL, which has been used in the calculations presented here.

The noise of the data is expected to be around or above 0.01 E for the diagonal components and much larger for the off-diagonal components. At the moment the characteristics of the noise is unknown, also because a pre-processing of the data is expected to remove the main part of the (correlated) noise. The calibration procedure will be considered as satisfactory if we are able to predict SGG data with an error below 20% (0.004 E) of the noise in the point-wise SGG measurements.

The “simple” LSC method was used for the tests concerning the size of the area and the resolution of the data, while the parametric LSC was used for the tests concerning the detection of systematic errors. Note, however, that systematic errors may be estimated directly by a comparison (regression analysis) between observed quantities and quantities computed from ground gravity.

The terrestrial gravity data sets used in this study are described in detail in section 5. As control data the realistic orbit of the IAG SC7 simulated data set was used. This data set comprises one month “clean” gravity gradient values from EGM96 to degree 300, referring to the right-handed instrument frame, aligned with the velocity vector and the z-axis lying in the plane formed by this vector and the position vector.

The precision of the calibration will be directly proportional to the gravity field (signal) standard deviation (see eq. 8) for example expressed as the standard deviation of gravity anomalies from which the contribution of a reference field have been subtracted. The areas studied here are therefore areas with a very smooth gravity field. The data, obviously, has to have a small noise, and should not contain systematic errors. In this study only data with a noise standard deviation below 2 mGal has been used. A part of this noise is correlated e.g. with noise due to the local height datum used for the computation of gravity anomalies. Assuming an error of 1m in the height datum, the correlated noise of gravity anomalies equals to 0.3 mgal.

We have used EGM96 to degree 360 for the reduction of gravity anomalies, in order to smooth as far as possible the gravity anomalies used in all test areas. Then, using the reduced gravity anomalies we have predicted gradient values at points selected from the SC7 simulated data set, further on called control values. To account for the errors of EGM96 (from degree 2 to 360) the error degree variances of EGM96 were added to the Legendre series formula used to express the covariance function (see eq. 9)

In order to compare the predicted with the control values, we have reduced also the control values using EGM96 to degree 360. In this way, the differences between control and predicted values are due to the spectral content of EGM96 between the degrees 301 and 360 and to the spectral content of the terrestrial gravity anomalies beyond degree 360. This procedure does not affect the calibration ability of our method, since dealing with simulated control data instead of real data we are based rather on the error estimation given by collocation instead of the statistics of the differences between the predicted and the control values. More specifically, we compute the mean collocation error, depending on the choice of the covariance function, as the mean of the formal LSC standard deviation of the predicted gravity gradient components, in order to draw conclusions about the optimal size of the area and the resolution of the data needed for the calibration. Note, however, that the error in the middle of the area typically is 90 % of the mean error, i.e. quantities located in the middle of the area are predicted with a smaller standard deviation than values at the borders.

It will be numerically shown in the next, that in all test areas, using LSC and terrestrial gravity anomalies, up to 80% of the formal standard deviation of the gravity gradient signal can be recovered, in the case of a high data accuracy, a large enough size of the area of collection of terrestrial gravity anomalies and a dense enough data-sampling. Furthermore, it will be also numerically shown that in this way it is possible to calibrate the GOCE SGG data for systematic errors such as bias and tilt.

In the computations the data-sampling and the size of the terrestrial data collections areas were kept constant as much as possible for the corresponding experiments from area to area.

5. GRAVITY DATA USED

For reasons discussed in earlier work (e.g. [RD-29]: Arabelos & Tscherning, 1998), for the requirements of the calibration, the terrestrial data have to be collected from areas with possibly a smooth free air gravity anomaly field. A further reason for this is to avoid topographic reductions to smooth the gravity field, due to errors that could be introduced to gravity anomalies from erroneous altitudes and density hypotheses. Another requirement was to collect data from extended regions in different geographic latitudes due to the dependence of the distribution of the GOCE data on the latitude. We did not take into account that the SSG error also depends on the latitude due to the functioning of the attitude control. For all these reasons, data from the Canadian plains, Australia and Scandinavia were used.

5.1 TERRESTRIAL FREE-AIR GRAVITY ANOMALIES FROM THE CANADIAN PLAINS

This data set was already described in ([RD-29]: Arabelos & Tscherning, 1998) and is further on called region A. In the present report the reduced values of free-air gravity anomalies to degree 360 were used shown in Fig. 1. The corresponding statistics are shown in Table 1. A conservative error estimate of 1 mGal was used. The error was regarded as uncorrelated.

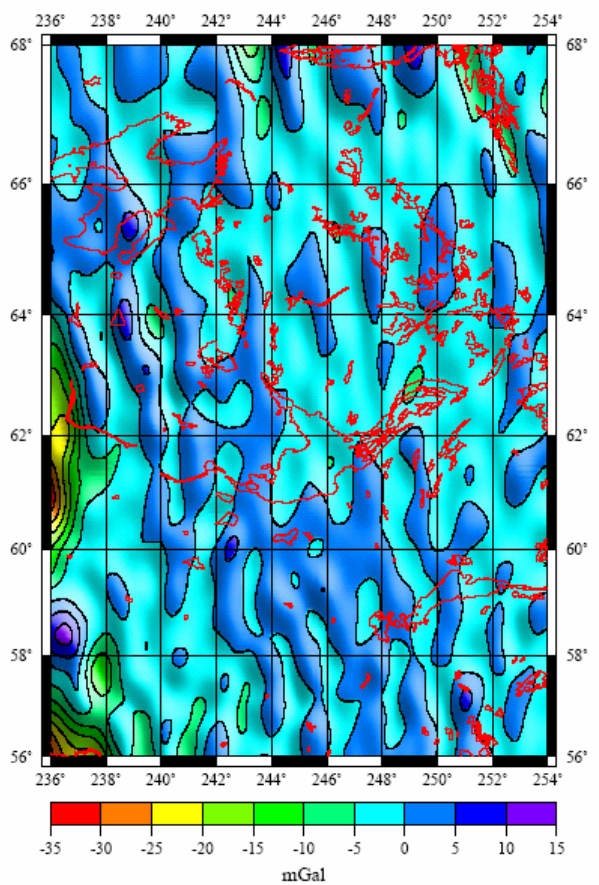

Fig. 1. The free-air anomaly-EGM96 gravity field in Canadian plains (smoothed)

Table 1. Statistics of the Canadian plains free-air gravity anomalies (14,177 point values)

	Observations	EGM96	Difference
Mean	-10.768	-10.678	-0.090
Standard Deviation	22.419	17.497	13.418
Max. Value	133.000	51.044	114.168
Minimum value	-81.100	-72.210	-124.857

5.2 SURFACE GRAVITY ANOMALIES FROM AUSTRALIA

The 2004 edition of the Australian National Gravity Database contains over 1,200,000 point values in the area bounded by $-48^0 \le \varphi \le -8^0$, $108^0 \le \lambda \le 162^0$ which is further called region B. This data was made available by Geoscience Australia. The data set covering the continental Australia and the surrounding ocean (1,117,054 point values) was reduced to EGM96. The statistics of the original and reduced free-air gravity anomalies are shown in Table 2.
As it is shown in Fig. 2 the gravity field is very smooth in central Australia and consequently, appropriate for the calibration requirements. For this reason, point gravity anomalies were selected from the area bounded by $-32^0 \le \varphi \le -20^0$, $124^0 \le \lambda \le 144^0$. A conservative error estimate of 1 mGal was used like in area A. The errors were also here regarded as uncorrelated.

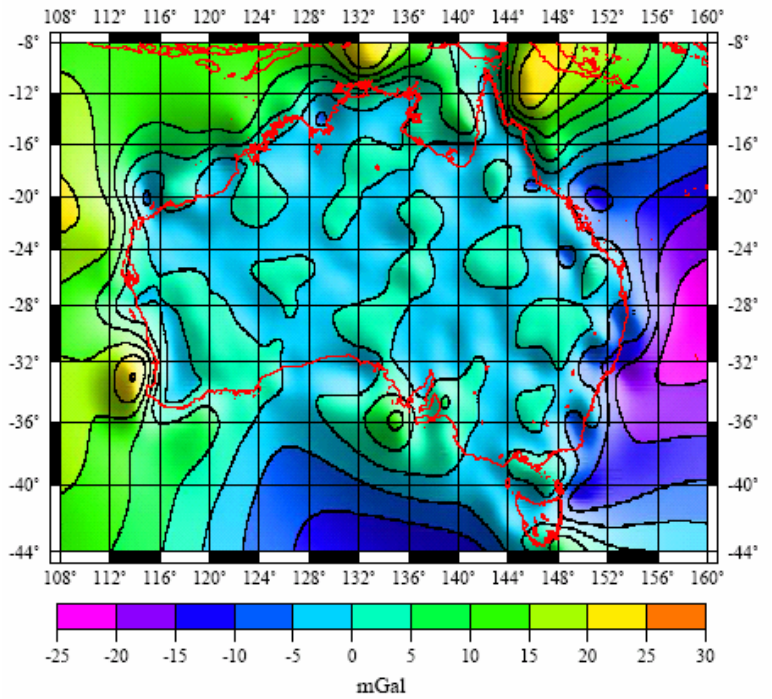

Figure 2. The free-air anomaly-EGM96 gravity field in Australia (smoothed)

Table 2. Statistics of the Australian free-air gravity anomalies

	Observations	EGM96	Difference
Mean	4.901	5.158	-0.258
Standard Deviation	24.504	22.504	12.102
Max. Value	248.602	94.223	219.875
Minimum value	-211.327	-104.930	-194.732

5.3 SURFACE GRAVITY ANOMALIES FROM SCANDINAVIA

Terrestrial as well as air-borne gravity anomaly data sets were made available by R. Forsberg, P. Knudsen and G. Strykovski (private communication). The terrestrial data set (62,126) covers the area $53.99^0 \leq \varphi \leq 64^0$, $11.97^0 \leq \lambda \leq 30.02^0$, further on called region C. After the reduction to EGM96 we obtain the statistics given in Table 3.

The air-borne data set covers the area $54.58^0 \leq \varphi \leq 60.12^0$, $12.01^0 \leq \lambda \leq 26.86^0$. The statistics of the air-borne gravity anomalies reduced to EGM96 (4,778 point values) are shown in Table 3. In the collocation experiments both data sets were used jointly with common accuracy equal to 2 mGal. The free-air gravity field reduced to EGM96 is shown in Fig. 3.

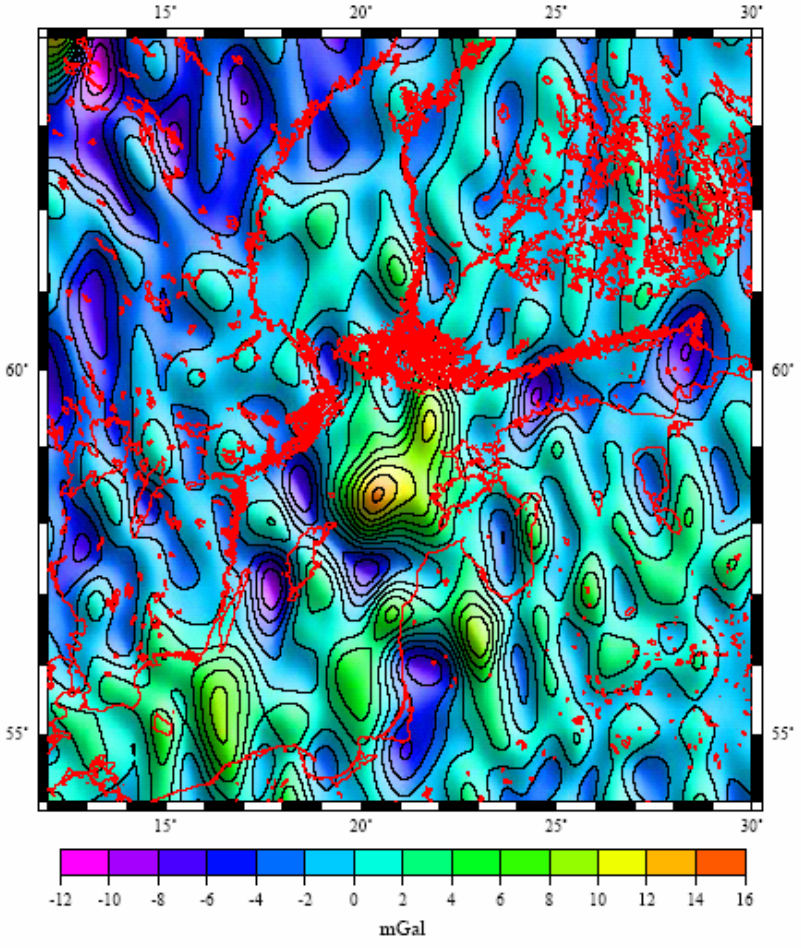

Figure 3. The combined (terrestrial and air-borne) free-air anomaly-EGM96 gravity field in Scandinavia (smoothed)

Table 3. Statistics of the terrestrial and airborne free-air gravity anomalies in Scandinavia

	Terrestrial observations	EGM96	Difference
Mean	-8.466	-8.118	-0.349
Standard Deviation	18.285	16.229	8.789
Max. Value	71.740	36.066	76.805
Minimum value	-84.021	-77.351	-47.250

	Air-borne observations	EGM96	Difference
Mean	-18.443	-19.735	1.292
Standard Deviation	19.834	18.209	10.024
Max. Value	29.660	21.235	35.085
Minimum value	-80.540	-68.107	-31.675

From Tables 1 to 3, it is shown that the reduced to EGM96 free-air gravity anomalies present very similar statistical characteristics. This is more evident from the shape of the corresponding covariance functions (see Figs.4, 5 and 7).

6.NUMERICAL EXPERIMENTS

The experiments concern recovery of 5 s sampling noise-free simulated GOCE data provided by IAG, along a 1 month realistic orbit (mean orbit altitude is 250 km), using terrestrial gravity anomalies. For the determination of the required size of the area for terrestrial data collection in all cases 10' data-sampling was used (values as close as possible to the middle of the area 10' cell were used) and prediction experiments were carried out in four areas with different size. For the determination of the required data-sampling, the prediction experiments were carried using data with 5, 7.5, 10, 15 and 20' sampling in areas with constant size.

The statistics of the gradient components used as control points in each of the three test areas is given in order to be able to compare with the statistics of the differences between control points and the corresponding predicted ones. In all computations the GRAVSOFT programs ([RD-35]: Tscherning et al., 1992) EMPCOV, COVFIT and GEOCOL were used.

6.1 REGION A

Simulated GOCE data used as control data in the area $58.5^0 \leq \varphi \leq 63.5^0$, $-118^0 \leq \lambda \leq -112^0$, (242 values). The statistics of these gravity gradient values are shown in Table 4. The covariance function used (empirical and corresponding analytical one) is shown in Figure 4.

Table 4. Statistics of the gravity gradient components used as control data in region (A). (EU)

	Mean value	Std. dev.	Min. value	Max. value
T_{xx}	0.1389	0.0598	-0.0136	0.2356
T_{xy}	0.0409	0.2321	-0.2521	0.3625
T_{xz}	-0.0706	0.1071	-0.2527	0.1241
T_{yy}	0.1215	0.0516	-0.0119	0.1959
T_{yz}	-0.0151	0.2915	-0.3869	0.3737
T_{zz}	-0.2605	0.0903	-0.4168	-0.0941

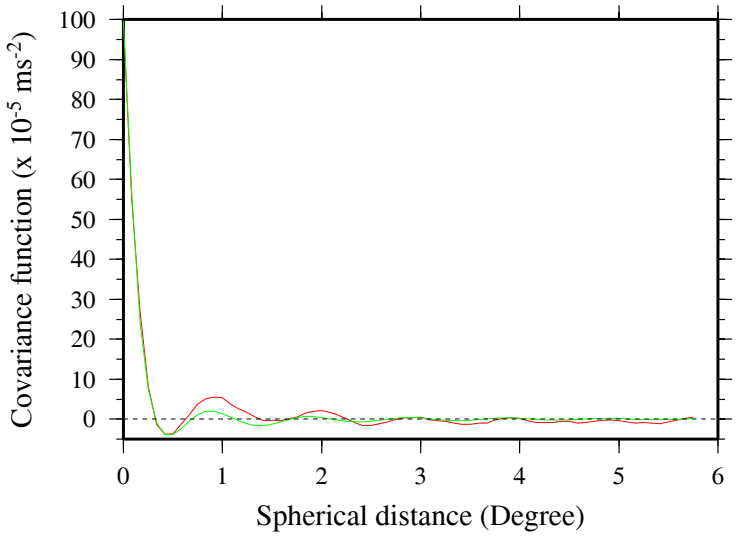

Fig.4. Covariance function of free-air gravity anomalies in the region (A) (red=empirical, green=model).

6.1.1 Determination of the size of the area for terrestrial data collection

The experiments were carried out using terrestrial gravity data with constant 10 min sampling. Accuracy equal to 1 mGal was adopted for these data. Prediction experiments were carried out collecting terrestrial data from four areas with size $5^0 \times 6^0$, $6^0 \times 8^0$, $8^0 \times 10^0$ and $10^0 \times 12^0$ respectively. The size of the first area corresponds to size of the control points collection area. The results of these numerical experiments are shown in Table 6.

The assessment of the prediction results in collocation is based not only on the statistics of the differences between observed (control) and predicted quantities, but also on the collocation error estimation of the prediction. It is well known that the actual standard deviation of the observed quantities remains constant, while the formal standard deviation (the square root of the variance of the signal covariance function used) and consequently the collocation error estimation depend on the covariance function. For this reason, the formal standard deviation of the control points as well as the mean error estimation (the mean value of the collocation error estimation over all predicted points) are given simultaneously with the statistics of the differences between control and predicted quantities (see Tables 5, 6, etc.). However, due to different spectral content between the control values and the gravity data used in our experiments the standard deviation of predicted-control values increases when the area increase, because more and more information above degree 360 is added, and the control values only contain information to degree 300, cf. the remarks given above. For this reason, the statistics of the differences between observed and predicted quantities cannot be used as criterion for the determination of the size of required areas but it is still useful to ascertain that the order of magnitude of our predictions is correct.

In Tables 5, 6, as well as in the relevant tables for the areas B and C, results are given for all the gravity gradient components. Since the behavior of the different components concerning the results is very similar, e.g. the error estimation is decreasing with increasing size of the collection area or with increasing data density, the discussion is mainly focused on T_{zz}, which is related more strictly to the gravity anomaly, than the other components.

With the increase of the collection area from $5^0 \times 6^0$ to $10^0 \times 12^0$, an improvement of the mean error estimation concerning all gradient components is shown in Table 5. This improvement is more significant in the case of T_{zz} (37%). The mean error of 0.0027 EU correspond to a 37% of the formal standard deviation of T_{zz}, resulting from the covariance function of free-air gravity anomalies in this region. This could be interpreted as the ability of the method to recover the 63% of the signal, in the case of real SGG data. On the other hand, the increased value of the standard deviation of the differences between control and predicted quantities represent only a small part (10.6%) of the standard deviation of the simulated control values (see Table 4), and as it was discussed in section 4 is due to the different resolution between the predicted and the simulated SGG control data.

Table 5. Results in terms of the statistics of the differences between predicted-control quantities in the region (A), concerning the determination of the size of required area with terrestrial gravity data. (Unit is EU). In the left column, in parenthesis, the formal standard deviation of the gravity gradient components referring to EGM96, and in the last column the mean collocation error (as computed by LSC) are shown.

Component	Mean value	Std. dev.	Min. value	Max. value	Mean coll. err.
$58.5^0 \le \varphi \le 63.5^0$, $-118^0 \le \lambda \le -112^0$ (859 point values)					
T_{xx} (0.0043)	0.0008	0.0041	-0.0057	0.0084	0.0031
T_{xy} (0.0050)	-0.0001	0.0027	-0.0073	0.0067	0.0040
T_{xz} (0.0051)	0.0003	0.0047	-0.0106	0.0122	0.0036
T_{yy} (0.0043)	0.0013	0.0026	-0.0034	0.0060	0.0030
T_{yz} (0.0051)	0.0005	0.0029	-0.0063	0.0063	0.0037
T_{zz} (0.0072)	-0.0021	0.0063	-0.0144	0.0090	0.0044
$58^0 \le \varphi \le 64^0$, $-119^0 \le \lambda \le -111^0$ (1414 point values)					
T_{xx} (0.0043)	0.0010	0.0044	-0.0067	0.0090	0.0026
T_{xy} (0.0050)	-0.0009	0.0034	-0.0091	0.0057	0.0036
T_{xz} (0.0051)	0.0005	0.0052	-0.0114	0.0128	0.0030
T_{yy} (0.0043)	0.0007	0.0033	-0.0055	0.0056	0.0026
T_{yz} (0.0051)	0.0006	0.0037	-0.0064	0.0074	0.0032
T_{zz} (0.0072)	-0.0017	0.0072	-0.0136	0.0115	0.0035
$57^0 \le \varphi \le 65^0$, $-120^0 \le \lambda \le -110^0$ (2385 point values)					
T_{xx} (0.0043)	0.0011	0.0058	-0.0085	0.0113	0.0023
T_{xy} (0.0050)	-0.0019	0.0038	-0.0088	0.0067	0.0031
T_{xz} (0.0051)	0.0006	0.0066	-0.0132	0.0150	0.0024
T_{yy} (0.0043)	0.0006	0.0038	0.0070	-0.0072	0.0022
T_{yz} (0.0051)	0.0010	0.0041	0.0080	-0.0084	0.0027
T_{zz} (0.0072)	-0.0017	0.0091	-0.0158	0.0146	0.0029
$56^0 \le \varphi \le 66^0$, $-121^0 \le \lambda \le -109^0$ (3578 point values)					
T_{xx} (0.0043)	0.0015	0.0058	-0.0088	0.0120	0.0020
T_{xy} (0.0050)	-0.0036	0.0046	-0.0119	0.0053	0.0026
T_{xz} (0.0051)	0.0006	0.0073	-0.0143	0.0157	0.0021
T_{yy} (0.0043)	0.0001	0.0045	-0.0092	0.0079	0.0020
T_{yz} (0.0051)	0.0011	0.0051	-0.0117	0.0095	0.0023
T_{zz} (0.0072)	-0.0016	0.0096	-0.0159	0.0161	0.0027

6.1.2 Determination of the required data-sampling

Concerning the determination of the data-sampling, experiments were carried out with terrestrial data collected from the same 6^0 x 8^0 area ($58^0 \le \varphi \le 64^0$, $-119^0 \le \lambda \le -111^0$) but with different resolution (5, 7.5, 10, 15 and 20 min). The results of these experiments are shown in Table 6.

Table 6. Results in terms of the statistics of the differences between predicted-control quantities from the experiments in the region (A), concerning the influence of the terrestrial gravity data-sampling. (Unit is EU)

Component	Mean value	Std. dev.	Min. value	Max. value	Mean coll. err.
Area: $58^0 \le \varphi \le 64^0$, $-119^0 \le \lambda \le -111^0$, Data-sampling 5' (2252 point values)					
T_{xx} (0.0043)	0.0010	0.0040	-0.0061	0.0085	0.0025
T_{xy} (0.0050)	-0.0011	0.0032	-0.0089	0.0053	0.0036
T_{xz} (0.0051)	0.0005	0.0048	-0.0110	0.0120	0.0029
T_{yy} (0.0043)	0.0008	0.0032	-0.0054	0.0057	0.0025
T_{yz} (0.0051)	0.0005	0.0037	-0.0066	0.0074	0.0031
T_{zz} (0.0072)	-0.0017	0.0067	-0.0128	0.0109	0.0032
Area: $58^0 \le \varphi \le 64^0$, $-119^0 \le \lambda \le -111^0$, Data-sampling 7.5' (1814 point values)					
T_{xx} (0.0043)	0.0010	0.0038	-0.0056	0.0083	0.0026
T_{xy} (0.0050)	-0.0011	0.0031	-0.0086	0.0051	0.0036
T_{xz} (0.0051)	0.0004	0.0046	-0.0111	0.0117	0.0030
T_{yy} (0.0043)	0.0009	0.0031	-0.0050	0.0057	0.0025
T_{yz} (0.0051)	0.0005	0.0035	-0.0062	0.0067	0.0032
T_{zz} (0.0072)	-0.0019	0.0064	-0.128	0.0100	0.0033
Area: $58^0 \le \varphi \le 64^0$, $-119^0 \le \lambda \le -111^0$, Data-sampling 10' (1414 point values)*					
T_{xx} (0.0043)	0.0010	0.0044	-0.0067	0.0090	0.0026
T_{xy} (0.0050)	-0.0009	0.0034	-0.0091	0.0057	0.0036
T_{xz} (0.0051)	0.0005	0.0052	-0.0114	0.0128	0.0030
T_{yy} (0.0043)	0.0007	0.0033	-0.0055	0.0056	0.0026
T_{yz} (0.0051)	0.0006	0.0037	-0.0064	0.0074	0.0032
T_{zz} (0.0072)	-0.0017	0.0072	-0.0136	0.0115	0.0035
Area: $58^0 \le \varphi \le 64^0$, $-119^0 \le \lambda \le -111^0$, Data-sampling 15' (743 point values)					
T_{xx} (0.0043)	0.0009	0.0043	-0.0061	0.0090	0.0029
T_{xy} (0.0050)	-0.0009	0.0030	-0.0075	0.0060	0.0038
T_{xz} (0.0051)	0.0004	0.0051	-0.0117	0.0125	0.0033
T_{yy} (0.0043)	0.0010	0.0029	-0.0045	0.0058	0.0029
T_{yz} (0.0051)	0.0006	0.0032	-0.0061	0.0058	0.0035
T_{zz} (0.0072)	-0.0019	0.0069	-0.0136	0.0102	0.0041
Area: $58^0 \le \varphi \le 64^0$, $-119^0 \le \lambda \le -111^0$, Data-sampling 20' (423 point values)					
T_{xx} (0.0043)	0.0013	0.0034	-0.0044	0.0071	0.0032
T_{xy} (0.0050)	0.0004	0.0027	-0.0072	0.0059	0.0040
T_{xz} (0.0051)	0.0002	0.0043	-0.0105	0.0106	0.0037
T_{yy} (0.0043)	0.0013	0.0026	-0.0031	0.0065	0.0032
T_{yz} (0.0051)	0.0005	0.0028	-0.0063	0.0075	0.0038
T_{zz} (0.0072)	-0.0026	0.0057	-0.0136	0.0068	0.0050

* The results for this area and data sampling are the same as the corresponding results for the same area and data-sampling of Table 5.

6.2 REGION B

Experiments were carried out with constant 10' data-sampling. An empirical covariance function was computed from the 10' gravity data covering the area $-32^0 \le \varphi \le -20^0$, $124^0 \le \lambda \le 144^0$ (Fig. 4).

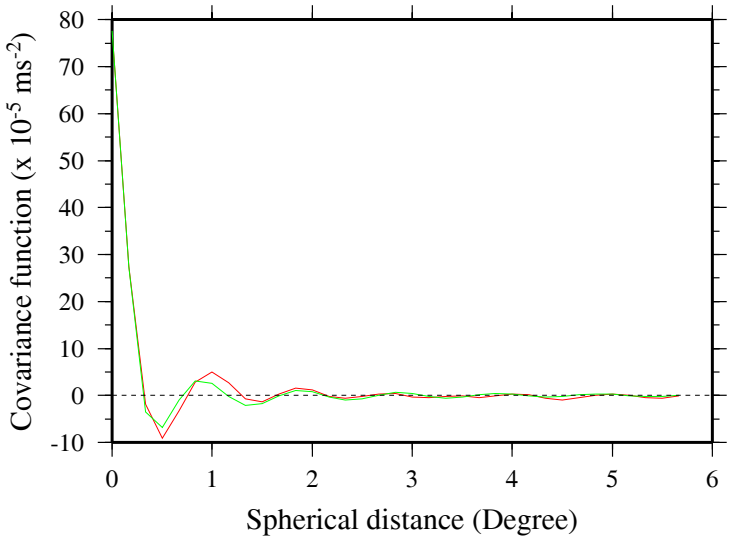

Fig. 5. Covariance function of free-air gravity anomalies in the region (B) (red=empirical, green=model)

The simulated GOCE data were collected from the area: $-30.5^0 \le \varphi \le -25.5^0$, $127^0 \le \lambda \le 133^0$ (245 values). The statistics of the gravity gradient components used as control data is shown in Table 7.

Table 7. The statistics of the gravity gradient components used as control data in the region (B). (EU)

	Mean value	Std. dev.	Min. value	Max. value
T_{xx}	0.1206	0.1058	-0.1137	0.2958
T_{xy}	0.0204	0.4166	-0.5133	0.5621
T_{xz}	0.0152	0.0240	-0.4630	0.4862
T_{yy}	0.1585	0.0748	0.0063	0.3120
T_{yz}	0.0286	0.1754	-0.3482	0.3390
T_{zz}	-0.2792	0.1675	-0.5499	0.0750

The terrestrial data were assumed to be accurate to 1 mGal. The simulated GOCE data were assumed to have accuracy equal to 0.001 EU. (The expected error is more than a factor 10 larger).

6.2.1 Determination of the size of the area for terrestrial data collection

The experiments were carried out using terrestrial gravity data with constant 10 min sampling. Prediction experiments were carried out collecting terrestrial data from four areas with size $5^0 \times 6^0$, $6^0 \times 8^0$, $8^0 \times 10^0$ and $10^0 \times 12^0$ respectively. The size of the first area corresponds to size of the control points collection area. The results of the prediction are shown in Table 9.

In the region B the formal standard deviation of T_{zz} is 0.0060 EU when the covariance function is computed from terrestrial gravity anomalies in the area $-32^0 \le \varphi \le -20^0$, $124^0 \le \lambda \le 144^0$, while it increases to 0.0089 EU when the covariance function is computed from terrestrial data in the area $-30.5^0 \le \varphi \le -25.5^0$, $127^0 \le \lambda \le 133^0$. The mean collocation error is like in 6.1 considered as a measure of the part of the real signal that could be recovered.

Table 8. Results in terms of the statistics of the differences between predicted-observed quantities in the region (B), concerning the determination of the size of required area with terrestrial gravity data. (Unit is EU). In the left column, in parenthesis, the formal standard deviation of the gravity gradient component, and in the last column the mean collocation error are shown.

$-30.5^0 \le \varphi \le -25.5^0$, $127^0 \le \lambda \le 133^0$ (1086 point values)					
Component	Mean value	Std. dev.	Min. value	Max. value	Mean coll. err.
T_{xx} (0.0036)	-0.0013	0.0042	-0.0108	0.0063	0.0024
T_{xy} (0.0041)	-0.0012	0.00390	-0.0095	0.0067	0.0032
T_{xz} (0.0042)	-0.0000	0.0053	-0.0119	0.0115	0.0028
T_{yy} (0.0036)	-0.0009	0.0033	-0.0090	0.0075	0.0024
T_{yz} (0.0042)	0.0003	0.0045	-0.0113	0.0096	0.0028
T_{zz} (0.0060)	0.0021	0.0068	-0.0128	0.0188	0.0032
$-31^0 \le \varphi \le -25^0$, $126^0 \le \lambda \le 134^0$ (1737 point values)					
T_{xx} (0.0036)	-0.0016	0.0053	-0.0127	0.0084	0.0019
T_{xy} (0.0041)	-0.0017	0.0036	-0.0089	0.0057	0.0027
T_{xz} (0.0042)	-0.0000	0.0058	-0.0147	0.0136	0.0022
T_{yy} (0.0036)	-0.0014	0.0033	-0.0081	0.0059	0.0019
T_{yz} (0.0042)	0.0004	0.0048	-0.0106	0.0087	0.0022
T_{zz} (0.0060)	0.0031	0.0077	-0.0141	0.0205	0.0023
$-32^0 \le \varphi \le -24^0$, $125^0 \le \lambda \le 135^0$ (2831 point values)					
T_{xx} (0.0036)	-0.0015	0.0068	-0.0170	0.0101	0.0016
T_{xy} (0.0041)	-0.0030	0.0045	-0.0119	0.0066	0.0021
T_{xz} (0.0042)	0.0000	0.0074	-0.0187	0.0182	0.0018
T_{yy} (0.0036)	-0.0019	0.0042	-0.0108	0.0072	0.0016
T_{yz} (0.0042)	0.0007	0.0061	-0.0136	0.0125	0.0017
T_{zz} (0.0060)	0.0034	0.0099	-0.0165	0.0274	0.0017
$-33^0 \le \varphi \le -23^0$, $124^0 \le \lambda \le 136^0$ (3879 point values)					
T_{xx} (0.0036)	-0.0006	0.0069	-0.0174	0.0118	0.0015
T_{xy} (0.0041)	-0.0044	0.0055	-0.0144	0.0066	0.0018
T_{xz} (0.0042)	0.0001	0.0088	-0.0210	0.0209	0.0016
T_{yy} (0.0036)	-0.0026	0.0046	-0.0129	0.0065	0.0015
T_{yz} (0.0042)	0.0009	0.0067	-0.0152	0.0151	0.0015
T_{zz} (0.0060)	0.0032	0.0104	-0.0172	0.0294	0.0018

In Table 8 it is shown that e.g. in the case of T_{zz}, the mean collocation error decreased from 53% to 30% of the formal standard deviation of T_{zz}, when the size of the collection of terrestrial data was increased from $5^0 \times 6^0$ to $10^0 \times 12^0$. On the other hand, the standard deviation between observed and predicted T_{zz} increased from 2.5% to 6.2% of the standard deviation of the control data. These numbers, even in the worst case of 6.2%, could be considered as fulfilling the requirements of the calibration procedure, see the introduction to the paper. The decision concerning the size of the area for the collection of terrestrial data has again been based on the mean collocation error. This means that with an area extent of $10^0 \times 12^0$ about 65% of the signal of the real data could be recovered.

6.2.2 Determination of the required data-sampling

Terrestrial gravity anomalies with data-sampling 5, 7.5, 10, 15 and 20 min were collected from the area bounded by $-31^0 \le \varphi \le -25^0$, $126^0 \le \lambda \le 134^0$. The prediction results are shown in Table 9.

Table 9. Results in terms of the statistics of the differences between predicted-observed quantities from the experiments in the region (B), concerning the influence of the terrestrial gravity data-sampling. (Unit is EU)

Component	Mean value	Std. dev.	Min. value	Max. value	Mean coll. err.
Area: $-31^0 \le \varphi \le -25^0$, $126^0 \le \lambda \le 134^0$, Data-sampling 5' (6090 point values)					
T_{xx} (0.0036)	-0.0009	0.0050	-0.0119	0.0088	0.0017
T_{xy} (0.0041)	-0.0015	0.0036	-0.0089	0.0060	0.0026
T_{xz} (0.0042)	0.0000	0.0055	-0.0146	0.0142	0.0021
T_{yy} (0.0036)	-0.0011	0.0034	-0.0075	0.0069	0.0018
T_{yz} (0.0042)	0.0004	0.0047	-0.0091	0.0080	0.0020
T_{zz} (0.0060)	0.0020	0.0074	-0.0155	0.0183	0.0018
Area: $-31^0 \le \varphi \le -25^0$, $126^0 \le \lambda \le 134^0$, Data-sampling 7.5' (3088 point values)					
T_{xx} (0.0036)	-0.0009	0.0053	-0.0124	0.0096	0.0018
T_{xy} (0.0041)	-0.0017	0.0038	-0.0095	0.0066	0.0026
T_{xz} (0.0042)	0.0000	0.0058	-0.0152	0.0146	0.0021
T_{yy} (0.0036)	-0.0010	0.0038	-0.0080	0.0080	0.0018
T_{yz} (0.0042)	0.0005	0.0050	-0.0093	0.0088	0.0021
T_{zz} (0.0060)	0.0019	0.0081	-0.0171	0.0195	0.0020
Area: $-31^0 \le \varphi \le -25^0$, $126^0 \le \lambda \le 134^0$, Data-sampling 10' (1737 point values)**					
T_{xx} (0.0036)	-0.0016	0.0053	-0.0127	0.0084	0.0019
T_{xy} (0.0041)	-0.0017	0.0036	-0.0089	0.0057	0.0027
T_{xz} (0.0042)	-0.0000	0.0058	-0.0147	0.0136	0.0022
T_{yy} (0.0036)	-0.0014	0.0033	-0.0081	0.0059	0.0019
T_{yz} (0.0042)	0.0004	0.0048	-0.0106	0.0087	0.0022
T_{zz} (0.0060)	0.0031	0.0077	-0.0141	0.0205	0.0023
Area: $-31^0 \le \varphi \le -25^0$, $126^0 \le \lambda \le 134^0$, Data-sampling 15' (773 point values)					
T_{xx} (0.0036)	-0.0007	0.0045	-0.0094	0.0091	0.0023
T_{xy} (0.0041)	-0.0019	0.0037	-0.0090	0.0058	0.0030
T_{xz} (0.0042)	0.0000	0.0052	-0.0130	0.0119	0.0027
T_{yy} (0.0036)	-0.0008	0.0037	-0.0068	0.0083	0.0023
T_{yz} (0.0042)	0.0003	0.0048	-0.0110	0.0090	0.0026
T_{zz} (0.0060)	0.0014	0.0073	-0.0171	0.0162	0.0032
Area: $-31^0 \le \varphi \le -25^0$, $126^0 \le \lambda \le 134^0$, Data-sampling 20' (436 point values)					
T_{xx} (0.0036)	-0.008	0.0027	-0.0079	0.0049	0.0028
T_{xy} (0.0041)	-0.0015	0.0021	-0.0061	0.0038	0.0034
T_{xz} (0.0042)	0.0000	0.0036	-0.0095	0.0098	0.0032
T_{yy} (0.0036)	-0.0008	0.0020	-0.0053	0.0041	0.0028
T_{yz} (0.0042)	0.0002	0.0024	-0.0060	0.0047	0.0032
T_{zz} (0.0060)	0.0015	0.0043	-0.0080	0.0132	0.0043

** The results for this area and data sampling are the same as the corresponding results for the same area and data-sampling of Table 9.

From Table 9 it is shown that the mean collocation error for the same size of the area of collection of terrestrial gravity anomalies decreased when the density of the data was increased, for all the gravity gradient components. In terms of percentage of the formal standard deviation of the various components this decrease is more significant in the case of T_{zz}, since it drops from 71% to 30% as the data-sampling changes from 20 to 5 min.

As it is shown in another experiment (see Table 10), a further increase of the size of the area in the case of 20' data-sampling, has no significant effect on the prediction results e.g. of T_{zz}.

Combining the results of Tables 8 and 9 it is reasonable to expect that using data in the larger area ($-33^0 \le \varphi \le -23^0$, $124^0 \le \lambda \le 136^0$) of Table 8 with the more dense data-sampling of Table

9 we will get the better results in terms of the formal mean error estimation. This was verified with a relevant experiment (see Table 11)

Table 10. Results of experiments in the region (B), showing that in the case of a coarse data-sampling the increase of the size of data collection area has no significant effect. (Unit is EU)

Area: $-33^0 \le \varphi \le -23^0$, $124^0 \le \lambda \le 136^0$, Data-sampling 20', (982 point values)					
Component	Mean value	Std. dev.	Min. value	Max. value	Mean coll. err.
T_{zz} (0.0060)	0.0009	0.0050	-0.0100	0.0173	0.0041
Area: $-32^0 \le \varphi \le -20^0$, $124^0 \le \lambda \le 144^0$, Data-sampling 20', (2163 point values)					
T_{zz} (0.0060)	0.0007	0.0050	-0.0110	0.0168	0.0041

Table 11. Results of prediction of T_{zz} (EU) in area (B), showing the improvement of the mean collocation error when terrestrial gravity anomalies with 7.5 and 5' sampling are used in the area $-33^0 \le \varphi \le -23^0$, $124^0 \le \lambda \le 136^0$

Area: $-33^0 \le \varphi \le -23^0$, $124^0 \le \lambda \le 136^0$, Data-sampling 7.5', (6834 point values)					
Component	Mean value	Std. dev.	Min. value	Max. value	Mean coll. err.
T_{zz} (0.0060)	0.0021	0.0111	-0.0206	0.0302	0.0014
Area: $-33^0 \le \varphi \le -23^0$, $124^0 \le \lambda \le 136^0$, Data-sampling 5', (13476 point values)					
T_{zz} (0.0060)	0.0025	0.011	-0.0194	0.0296	0.0012

Finally, the ability of the method was evaluated with respect to the detection of systematic errors in the GOCE data. For this reason, the data used earlier as control data was added to the 7.5 min sampled terrestrial gravity data in the area $-31^0 \le \varphi \le -25^0$, $126^0 \le \lambda \le 134^0$. However, it was assumed that they were affected by systematic errors, as it is expected for the real SGG measurements (The data were used as point data, but it is possible to use low-pass filtered data also). This corresponds to the use of eq. (3) (Torge, 2001). After the exclusion of two very short tracks that included only 6 and 8 points respectively, the data set consists of 233 T_{zz} values distributed over 16 tracks (see Fig.6).

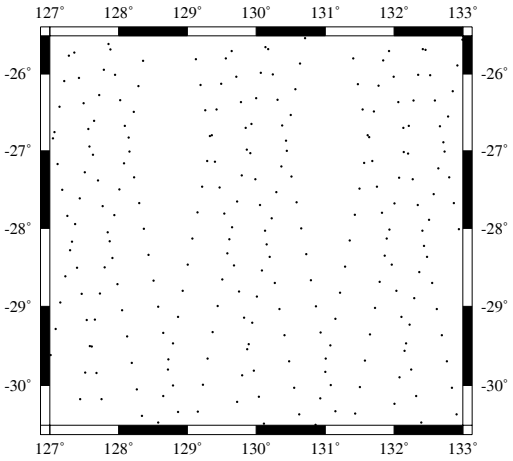

Figure 6. Additional input data (16 GOCE tracks) used in the experiment for the estimation of systematic errors

For each of them two parameters, a bias and a tilt were estimated. The results of this experiment in terms of the parameters and their error estimates are shown in Table 12. Concerning the tilt, almost zero values were found with very high accuracy, while the error estimates for the bias does not exceed 33% of the formal standard deviation of T_{zz}. Form the table one may get the impression that some estimated biases are significantly different from zero. However, this is again caused by the fact that the used gravity gradient data only

contains information up to degree 300, while the computed quantities in principle contains information up to infinity.

Table 12. Results of the estimation of systematic errors using parametric collocation

Track No.	Bias (EU)	Error of estimation	Tilt (10^{-7} EU/s)	Error of Estimation
1	-0.0020	0.0021	0.12	0.66
2	0.0050	0.0016	-2.64	6.55
3	0.0046	0.0016	3.69	6.09
4	0.0017	0.0016	-0.42	6.55
5	-0.0006	0.0016	3.74	6.19
6	-0.0001	0.0020	-0.13	0.43
7	0.0011	0.0017	2.69	6.07
8	0.0061	0.0016	-4.34	6.64
9	0.0040	0.0015	1.71	6.00
10	-0.0015	0.0016	-3.33	6.69
11	-0.0016	0.0017	5.58	6.19
12	0.0017	0.0017	-0.15	0.42
13	0.0025	0.0016	3.11	6.00
14	0.0060	0.0016	-7.56	6.74
15	0.0028	0.0015	0.14	5.98
16	-0.0042	0.0018	-5.45	6.93

6.3 REGION C

The empirical covariance function was computed from gravity data covering the area $54^0 \leq \varphi \leq 64^0$, $12^0 \leq \lambda \leq 30^0$. This is shown in Fig. 6 together with its analytical fitting.

Simulated GOCE data were collected from the area bounded by $57^0 \leq \varphi \leq 62^0$, $21^0 \leq \lambda \leq 27^0$ (250 values) in order to be used as control data. For these data accuracy equal to 0.001 EU was adopted. The statistics of the simulated GOCE data used as control values are shown in Table 14.

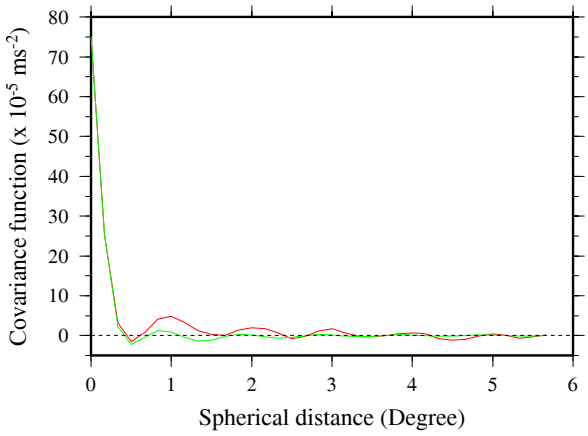

Fig. 7. Covariance function of free-air gravity anomalies in the region (C) (red=empirical, green=model).

Table 13. The statistics of the gravity gradient components used as control data in the region (C). (EU)

	Mean value	Std. dev.	Min. value	Max. value
T_{xx}	0.1340	0.0303	0.0525	0.2076
T_{xy}	0.0358	0.0574	-0.0979	0.2291
T_{xz}	0.0019	0.0842	-0.1919	0.1921
T_{yy}	0.1249	0.0724	-0.0080	0.3200
T_{yz}	-0.0137	0.0525	-0.1076	0.1200
T_{zz}	-0.2590	0.0826	-0.4653	-0.0836

6.3.1 Determination of the size of the area for terrestrial data collection

The experiments were carried out using terrestrial gravity data with constant 10 min sampling. An accuracy equal to 2 mGal was adopted for these data. Prediction experiments were carried out collecting terrestrial data from four areas with size $5^0 \times 6^0$, $7^0 \times 8^0$, $9^0 \times 10^0$ and $10^0 \times 12^0$ respectively. The size of the first area corresponds to size of the control points collection area. The results of these numerical experiments are shown in Table 14.

Table 14. Results in terms of the statistics of the differences between predicted-control quantities in the region (C), concerning the determination of the size of required area with terrestrial gravity data. (Unit is EU). In the first column (in parenthesis) the formal standard deviation of the corresponding gravity gradient component is shown. In the last column the mean collocation error is shown.

Component	Mean value	Std. dev.	Min. value	Max. value	Mean coll. err.
$57^0 \le \varphi \le 62^0$, $21^0 \le \lambda \le 27^0$ (1072 point values)					
T_{xx} (0.0047)	0.0012	0.0032	-0.0036	0.0100	0.0032
T_{xy} (0.0055)	-0.0003	0.0035	-0.0090	0.0060	0.0043
T_{xz} (0.0056)	0.0004	0.0044	-0.0117	0.0107	0.0037
T_{yy} (0.0047)	0.0010	0.0034	-0.0045	0.0094	0.0031
T_{yz} (0.0056)	0.0000	0.0037	-0.0087	0.0101	0.0039
T_{zz} (0.0080)	-0.0022	0.0057	-0.0170	0.0077	0.0043
$56^0 \le \varphi \le 63^0$, $20^0 \le \lambda \le 28^0$ (1984 point values)					
T_{xx} (0.0047)	0.0022	0.0064	-0.0069	0.0164	0.0026
T_{xy} (0.0055)	0.0009	0.0062	-0.0120	0.0111	0.0037
T_{xz} (0.0056)	0.0013	0.0075	-0.0161	0.0184	0.0028
T_{yy} (0.0047)	0.0023	0.0066	-0.0075	0.0187	0.0023
T_{yz} (0.0056)	0.0005	0.0073	-0.0129	0.0169	0.0031
T_{zz} (0.0080)	-0.0040	0.0111	-0.0306	0.0109	0.0029
$55^0 \le \varphi \le 64^0$, $19^0 \le \lambda \le 29^0$ (3167 point values)					
T_{xx} (0.0047)	0.0019	0.0071	-0.0088	0.0164	0.0021
T_{xy} (0.0055)	0.0016	0.0066	-0.0115	0.0119	0.0031
T_{xz} (0.0056)	0.0016	0.0083	-0.0169	0.0193	0.0022
T_{yy} (0.0047)	0.0020	0.0068	-0.0088	0.0187	0.0020
T_{yz} (0.0056)	0.0007	0.0079	-0.0136	0.0183	0.0026
T_{zz} (0.0080)	-0.0039	0.0122	-0.0323	0.0142	0.0023
$54^0 \le \varphi \le 64^0$, $18^0 \le \lambda \le 30^0$ (4165 point values)					
T_{xx} (0.0047)	0.0016	0.0071	-0.0089	0.0157	0.0019
T_{xy} (0.0055)	0.0010	0.0066	-0.0122	0.0114	0.0026
T_{xz} (0.0056)	0.0016	0.0086	-0.0164	0.0189	0.0019
T_{yy} (0.0047)	0.0022	0.0068	-0.0091	0.0189	0.0018
T_{yz} (0.0056)	0.0008	0.0079	-0.0130	0.0181	0.0022
T_{zz} (0.0080)	-0.0038	0.0122	-0.0309	0.0149	0.0022

These results are very similar to the previous ones in Tables 6 and 9. Increasing the collection area from $5^0 \times 6^0$ to $10^0 \times 12^0$, the mean error estimation, e.g. in the case T_{zz} decreased up to 51% of its original value. In terms of percentage on the formal standard deviation of T_{zz} the mean estimation error drops from 53.8% to 27.5%.

6.3.2 Determination of the required data-sampling

For this purpose terrestrial gravity anomalies with data-sampling 5, 7.5, 10, 15 and 20 min were collected from the area bounded by $56^0 \le \varphi \le 63^0$, $20^0 \le \lambda \le 28^0$. The prediction results are shown in Table 15.

Table 15. Results in terms of the statistics of the differences between predicted-observed quantities from the experiments in the region (C), concerning the influence of the terrestrial gravity data-sampling. (Unit EU). In the first column (in parenthesis) the formal standard deviation of the corresponding gravity gradient component is shown. In the last column the mean collocation error is shown.

Component	Mean value	Std. dev.	Min. value	Max. value	Mean coll. err.
Area: $56^0 \le \varphi \le 63^0$, $20^0 \le \lambda \le 28^0$, Data-sampling 5' (7404 point values)					
T_{xx} (0.0047)	0.0021	0.0072	-0.0078	0.0175	0.0024
T_{xy} (0.0055)	0.0008	0.0065	-0.0121	0.0107	0.0036
T_{xz} (0.0056)	0.0014	0.0082	-0.0172	0.0199	0.0026
T_{yy} (0.0047)	0.0021	0.0069	-0.0083	0.0192	0.0022
T_{yz} (0.0056)	0.0006	0.0078	-0.0136	0.0184	0.0030
T_{zz} (0.0080)	-0.0042	0.0125	-0.0335	0.0125	0.0025
Area: $56^0 \le \varphi \le 63^0$, $20^0 \le \lambda \le 28^0$, Data-sampling 7.5' (3488 point values)					
T_{xx} (0.0047)	0.0022	0.0070	-0.0078	0.172	0.0025
T_{xy} (0.0055)	0.0007	0.0064	-0.0119	0.0101	0.0036
T_{xz} (0.0056)	0.0014	0.0082	-0.0171	0.0197	0.0027
T_{yy} (0.0047)	0.0024	0.0067	-0.0080	0.0188	0.0022
T_{yz} (0.0056)	0.0006	0.0077	-0.0128	0.0176	0.0030
T_{zz} (0.0080)	-0.0046	0.0123	-0.0330	0.0113	0.0026
Area: $56^0 \le \varphi \le 63^0$, $20^0 \le \lambda \le 28^0$, Data-sampling 10' (1984 point values)***					
T_{xx} (0.0047)	0.0022	0.0064	-0.0069	0.0164	0.0026
T_{xy} (0.0055)	0.0009	0.0062	-0.0120	0.0111	0.0037
T_{xz} (0.0056)	0.0013	0.0075	-0.0161	0.0184	0.0028
T_{yy} (0.0047)	0.0023	0.0066	-0.0075	0.0187	0.0023
T_{yz} (0.0056)	0.0005	0.0073	-0.0129	0.0169	0.0031
T_{zz} (0.0080)	-0.0040	0.0111	-0.0306	0.0109	0.0029
Area: $56^0 \le \varphi \le 63^0$, $20^0 \le \lambda \le 28^0$, Data-sampling 15' (894 point values)					
T_{xx} (0.0047)	0.0012	0.0066	-0.0078	0.0160	0.0028
T_{xy} (0.0055)	0.0006	0.0057	-0.0111	0.0091	0.0038
T_{xz} (0.0056)	0.0011	0.0075	-0.0144	0.0184	0.0031
T_{yy} (0.0047)	0.0008	0.0058	-0.0081	0.0160	0.0027
T_{yz} (0.0056)	0.0008	0.0065	-0.0119	0.0165	0.0034
T_{zz} (0.0080)	-0.0021	0.0112	-0.0272	0.0134	0.0037
Area: $56^0 \le \varphi \le 63^0$, $20^0 \le \lambda \le 28^0$, Data-sampling 20' (506 point values)					
T_{xx} (0.0047)	0.0008	0.0043	-0.0064	0.0090	0.0032
T_{xy} (0.0055)	0.0014	0.0042	-0.0082	0.0080	0.0041
T_{xz} (0.0056)	0.0007	0.0043	-0.0061	0.0118	0.0031
T_{yy} (0.0047)	0.0007	0.0043	-0.0061	0.0118	0.0031
T_{yz} (0.0056)	0.0006	0.0047	-0.0092	0.0118	0.0038
T_{zz} (0.0080)	-0.0015	0.0038	-0.0186	0.0094	0.0046

*** The results for this area and data sampling are the same as the corresponding results for the same area and data-sampling of Table 15.

Also these results are similar to the results of corresponding experiments in the regions A and B. The results are discussed in details in section 7.

7. SUMMARY AND CONCLUSION

Extended prediction experiments were carried out using terrestrial gravity anomalies from the Canadian plains, from Australia and from Scandinavia, in order to determine the appropriate size of the area for gravity data collection as well as the required data-sampling for calibration of the GOCE SGG data. A conservative estimate of 2 mGal for the standard deviation of the noise in the gravity data was used. The errors were considered uncorrelated.

In the following tables the results of the experiments in all areas (A, B and C) are summarized, expressed in terms of the percentage decrease of the mean collocation error when the size of the collection area is increasing from $5^0 \times 6^0$ to $10^0 \times 12^0$ (Table 16) and when the data sampling is increasing from 20′ to 5′ (Table 17).

Table 16. Percentage decrease of the mean collocation error, by increasing the size of the collection area from $5^0 \times 6^0$ to $10^0 \times 12^0$.

Area	T_{xx}	T_{xy}	T_{xz}	T_{yy}	T_{yz}	T_{zz}
A	35.5	35.0	41.6	33.3	37.8	38.6
B	37.5	43.8	42.9	37.5	46.4	43.8
C	40.6	39.5	48.6	41.9	43.6	48.8
Average	37.9	39.4	44.4	37.6	42.6	43.7

In Tables 5, 8 and 14 a continuous decrease of the mean collocation error is shown with increasing size of the data collection area. As it is shown in Table 16 this is more intense in the areas B and C, and in average, concern gradients including derivatives with respect to z.

Table 17. Percentage decrease of the mean collocation error, by increasing the data sampling from 20′ to 5′.

Area	T_{xx}	T_{xy}	T_{xz}	T_{yy}	T_{yz}	T_{zz}
A	21.9	10.0	21.6	21.9	18.4	36.0
B	39.3	23.5	34.4	35.7	37.5	58.1
C	25.0	12.2	16.1	29.0	21.0	45.7
Average	28.7	15.2	24.0	28.9	25.6	46.6

In Tables 6, 9 and 15 there is also a continuous decrease of the mean collocation error with increasing data sampling. In Table 17 it is shown that the decrease is more intense for all components in the area B and concern especially the vertical gravity gradient.

In the following tables the results of the experiments in all areas (A, B and C) are summarized, expressed in terms of the mean collocation error as percentage of the formal standard deviation of the corresponding gravity gradient components for optimal size of the data collection area (equal to $10^0 \times 12^0$) (Table 18) and for optimal data sampling (equal to 5′) (Table 19).

Table 18. Mean collocation error as percentage of the formal standard deviation in experiments with a size of the area for data collection equal to $10^0 \times 12^0$.

Area	T_{xx}	T_{xy}	T_{xz}	T_{yy}	T_{yz}	T_{zz}
A	46.5	52.0	41.2	46.5	45.1	37.5
B	41.7	43.9	38.1	41.7	35.7	30.0
C	40.4	47.3	33.9	38.3	39.3	27.5
Average	42.9	47.7	37.7	42.2	40.0	31.7

Table 19. Mean collocation error as percentage of the formal standard deviation in experiments with a data sampling equal to 5′.

Area	T_{xx}	T_{xy}	T_{xz}	T_{yy}	T_{yz}	T_{zz}
A	58.1	72.0	56.9	58.1	60.8	44.4
B	47.2	63.4	50.0	50.0	47.6	30.0
C	51.1	65.5	46.4	46.8	53.6	31.3
Average	52.1	67.0	51.1	51.6	54.0	35.2

In Table 18 mean collocation errors ranging from 48% to 32% (average over all areas) of the formal standard deviation of the gravity gradient components are shown for the optimal size of the data collection area. Especially for T_{zz} the mean collocation error in Areas B and C drops down to 30% of the corresponding formal standard deviation. This means that a 70% of the signal of the real data can be recovered by the method used.

The corresponding percentage values for the optimal data sampling (Table 19) ranges from 67% to 35.2% in average, with T_{zz} showing again the smaller mean collocation error.

Finally in the area B an experiment, with simultaneously optimal size and optimal data sampling, resulted in a mean collocation error equal to 20% of the formal standard deviation for the component T_{zz}. In this case an 80% of the signal of the real data can be recovered by the method used.

Using parametric LSC it was shown that the estimation of systematic errors such as bias and tilt in the SGG data is possible using a combination of terrestrial with satellite data.

It is also possible to determine a scale factor for the total gravity gradients and it has also been implemented in the GRAVSOFT program GEOCOL. An off-line estimation of scale-factors, which has been used for CHAMP accelerometer data ([RD-31]: Howe et al., 2003) may, however, also be used.